Organ-Confined Prostate Cancer: Effect of Prior Transrectal Biopsy on Endorectal MRI and MR Spectroscopic Imaging

Aliya Qayyum[1]
Fergus V. Coakley[1]
Ying Lu[1]
Jeffrey D. Olpin[1,2]
Louis Wu[1]
Benjamin M. Yeh[1]
Peter R. Carroll[3]
John Kurhanewicz[1]

OBJECTIVE. Our aim was to determine the effect of prior transrectal biopsy on endorectal MRI and MR spectroscopic imaging findings in patients with organ-confined prostate cancer.

MATERIALS AND METHODS. Endorectal MRI and MR spectroscopic imaging were performed in 43 patients with biopsy-proven prostate cancer before radical prostatectomy confirming organ-confined disease. For each sextant, two independent reviewers scored the degree of hemorrhage on a scale from 1 to 5 and recorded the presence or absence of capsular irregularity. A spectroscopist recorded the number of spectrally degraded voxels in the peripheral zone. The outcome variables of capsular irregularity and spectral degradation were correlated with the predictor variables of time from biopsy and degree of hemorrhage after biopsy.

RESULTS. Capsular irregularity was unrelated to time from biopsy or to degree of hemorrhage. Spectral degradation was inversely related to time from biopsy ($p < 0.01$); the mean percentage of degraded peripheral zone voxels was 18.5% within 8 weeks of biopsy compared with 7% after 8 weeks. Spectral degradation was unrelated to the degree of hemorrhage.

CONCLUSION. In organ-confined prostate cancer, capsular irregularity can be seen at any time after biopsy and is independent of the degree of hemorrhage, whereas spectral degradation is seen predominantly in the first 8 weeks after biopsy. MRI staging criteria and guidelines for scheduling studies after biopsy may require appropriate modification.

The American Cancer Society estimated that there would be 230,110 new cases of prostate cancer and 29,900 deaths due to prostate cancer in the United States in 2004 [1]. Tumor extension beyond the prostate gland is an important histopathologic finding that influences staging, prognosis, and treatment [2–4]. Endorectal MRI can accurately detect extracapsular extension and seminal vesicle invasion, particularly when used in conjunction with MR spectroscopic imaging or analyzed with serum prostate-specific antigen levels [4–7]. It has been suggested that the magnitude and extent of metabolic abnormality on MR spectroscopic imaging may be indicative of tumor aggressiveness and stage [8, 9]. Many centers in the United States are now routinely performing MRI and MR spectroscopic imaging of the prostate, and an American College of Radiology Imaging Network multiinstitutional trial has been initiated. Despite such enthusiasm, hemorrhage after biopsy is a substantial limitation of MRI and MR spectroscopic imaging, resulting in both over- and underestimation of tumor extent [10–12]. The timing of MRI and MR spectroscopic imaging of the prostate after transrectal biopsy is therefore important. Prior studies have recommended an interval of 3 weeks between transrectal biopsy and MRI [2, 12–14]. Recently, there has been a trend toward increased prostate sampling during transrectal biopsy; currently, greater than six core biopsies are frequently obtained [15]. The increase in prostate sampling has raised new questions about the optimal timing of MRI and MR spectroscopic imaging after transrectal biopsy and the impact of hemorrhage after biopsy on the interpretation of MRI and MR spectroscopic imaging. Therefore, we undertook this study to determine the effect of prior transrectal biopsy on endorectal MRI and MR spectroscopic imaging findings in organ-confined prostate cancer.

Materials and Methods

Patients

This was a retrospective single-institutional study. The patients were recruited as part of an ongoing National Institutes of Health study investigating the use of MRI in patients with prostate cancer. The study re-

Received July 28, 2003; accepted after revision March 26, 2004.

[1]Department of Radiology, University of California, San Francisco, 505 Parnassus Ave., San Francisco, CA 94143-0628. Address correspondence to A. Qayyum.

[2]Present address: Department of Radiology, University of Utah, 30 N 1900 East, #1A71, Salt Lake City, UT 84132-2140.

[3]Department of Urology, University of California, San Francisco, San Francisco, CA 94143-0628.

AJR 2004;183:1079–1083

0361–803X/04/1834–1079

ceived approval from the institutional committee on human research, and written informed consent was obtained. We included all patients with organ-confined prostate cancer who underwent radical prostatectomy over a 1-year period and who had preoperative endorectal MRI and MR spectroscopic imaging of the prostate gland at our institution (n = 43). We limited the study to patients with organ-confined prostate cancer because they constitute most patients undergoing radical prostatectomy at our institution and because we wished to study prostate biopsy changes that might mimic extracapsular extension and to determine whether capsular irregularity may occur as a normal variant in organ-confined prostate cancer without confounding real extracapsular extension. The patients had prostate cancer proven on transrectal biopsy performed before MRI and MR spectroscopic imaging (mean interval, 8 weeks from biopsy to MRI and MR spectroscopic imaging; range, 2–17 weeks). Thirteen of the 43 patients underwent transrectal biopsy at our institution, and 30 patients underwent transrectal biopsy at outside institutions. The mean number of core biopsies was seven (range, five to 18). The median tumor Gleason score was 6 (range, 5–9). The mean prostate-specific antigen level at diagnosis was 6.6 ng/mL (range, 1.6–19.3 ng/mL). The mean patient age was 57 years (range, 44–75 years). None of the patients received preoperative hormonal or radiation therapy.

Imaging Technique

MRI was performed on a 1.5-T whole-body MRI scanner (Signa, GE Healthcare). The details of the MRI technique have been previously described [16, 17]. Patients were examined using the body coil for excitation and a pelvic phased-array coil in combination with a commercially available balloon-covered expandable endorectal coil for signal reception. Axial spin-echo T1-weighted images were obtained from the aortic bifurcation to the symphysis pubis, using the following parameters: TR/TE, 700/8; slice thickness, 5 mm; interslice gap, 1 mm; field of view, 24 cm; matrix, 256 × 192; frequency direction, transverse (to prevent obscuration of pelvic nodes by motion artifact of the endorectal coil); and 1 excitation. Thin-section high-spatial-resolution axial and coronal T2-weighted fast spin-echo images of the prostate and seminal vesicles were obtained using the following parameters: TR/TE_{eff}, 5,000/96; echo-train length, 16; slice thickness, 3 mm; interslice gap, 0 mm; field of view, 14 cm; matrix, 256 × 192; frequency direction, anteroposterior (to prevent obscuration of the prostate by motion artifact of the endorectal coil); and 3 excitations. All MR images were routinely postprocessed to compensate for the reception profile of the endorectal and pelvic phased-array coils [18]. After review of the axial T2-weighted images, a spectroscopic imaging volume was selected by an experienced spectroscopist in conjunction with a technologist to maximize coverage of the prostate, while minimizing inclusion of periprostatic fat and rectal air. MR spectroscopic imaging of the peripheral zone is only routinely performed because of limitations in gland coverage and the variable metabolic spectra in the transition zone attributed to stromal and glandular hyperplasia in benign prostatic hyperplasia [16].

Three-dimensional MR spectroscopic imaging data were acquired using a water- and lipid-suppressed double spin-echo point-resolved spectroscopic imaging sequence optimized for the quantitative detection of both choline and citrate [16]. Water and lipid suppression was achieved using the band-selective inversion with a gradient dephasing technique [19]. Outer voxel saturation pulses were also used to improve volume selection, to eliminate contamination from periprostatic fat, and to reduce susceptibility problems due to the rectal air–tissue interface [20]. Data sets were acquired as 16 × 8 × 8 phase-encoded spectral arrays (1,024 voxels) with a nominal spectral resolution of 0.24–0.34 cm^3 (TR/TE, 1,000/130; acquisition time, 17 min). The total examination time was 1 hr, including coil placement and patient positioning.

Image Interpretation

Two independent attending radiologists with subspecialty interest in abdominal and prostate MRI and MR spectroscopic imaging retrospectively reviewed the MR images of all 43 patients. Reviewers were aware that patients had prostate cancer but were unaware of all other clinical and histopathologic findings. In particular, reviewers were not aware that only patients with organ-confined disease were included. The reviewers recorded the degree of visible hemorrhage in the peripheral zone for each sextant on T1-weighted images using a 5-point scale where 0 indicated no hemorrhage, 1 indicated hemorrhage involving less than 25% of a sextant, 2 indicated hemorrhage involving 25–49% of a sextant, 3 indicated hemorrhage involving 50–75% of a sextant, and 4 indicated hemorrhage involving greater than 75% of a sextant. In addition, the sum of the hemorrhage score in each sextant was used to give a hemorrhage score for each patient. A total hemorrhage score was then obtained for each patient by combining the scores for both reviewers.

On T2-weighted images, both reviewers documented the presence or absence of capsular irregularity, loss of the rectoprostatic angle, and neurovascular bundle involvement for each sextant and also recorded the presence or absence of seminal vesicle invasion [5]. Capsular irregularity was defined as spiculated or streaky low signal intensity extending from the capsule (Fig. 1), low signal intensity in the periprostatic tissue, or focal irregular bulging of the capsule.

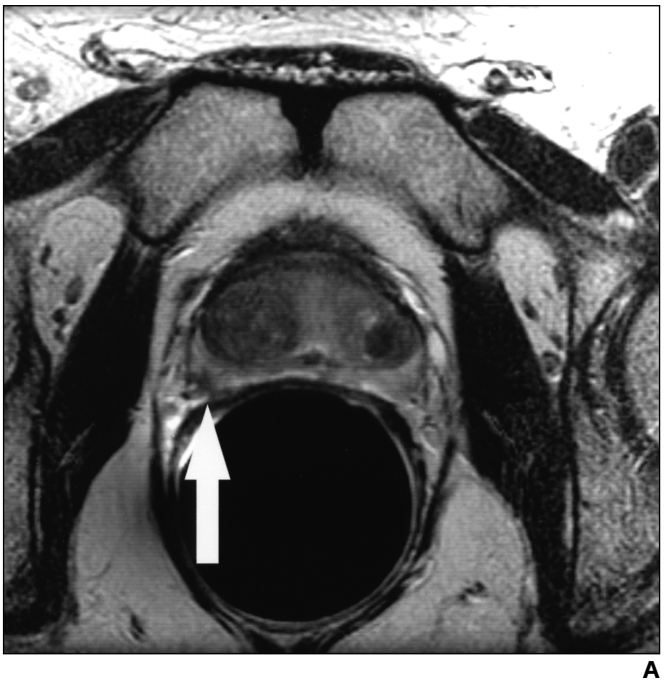

A

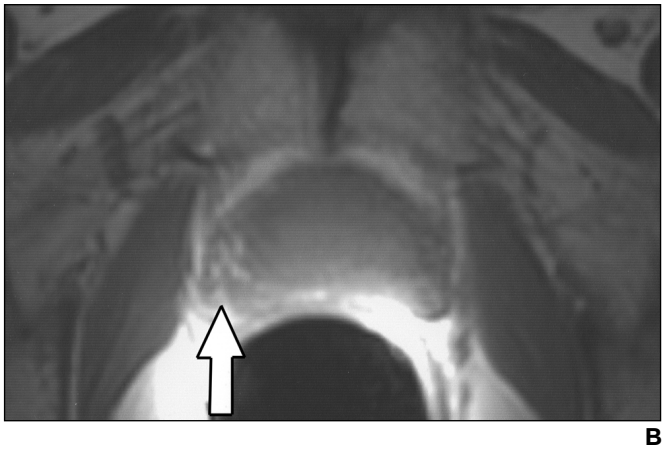

B

Fig. 1.—50-year-old man with mean prostate-specific antigen level of 17.6 ng/mL and positive transrectal biopsy indicating Gleason-score-6 tumor at right base and mid gland. **A,** Thin-section high-spatial-resolution axial T2-weighted image (TR/TE_{eff}, 5,000/96; slice thickness, 3 mm; interslice gap, 0 mm; field of view, 14 cm) shows spiculated low-signal-intensity change extending from prostate capsule at right base (*arrow*). **B,** Axial T1-weighted image (TR/TE, 700/8; slice thickness, 5 mm; interslice gap, 1 mm; field of view, 24 cm) shows high-signal-intensity hemorrhage in peripheral zone of right base (*arrow*) after biopsy.

The MR spectroscopic imaging data were overlaid on the corresponding axial T2-weighted images and evaluated by an experienced spectroscopist to determine those voxels in the peripheral zone that were unsuitable for analysis because of spectral degradation. Two spectral changes were associated with hemorrhage: The first was defined as a reduction in citrate but not choline and creatine because most of the citrate is in the ducts in which the blood collects. The second was an overall loss of all metabolites due to both a reduction in cell density and the blood occupying part or all of the spectroscopic voxel and spectral line broadening due to the presence of deoxyhemoglobin. Voxels were considered spectrally degraded by hemorrhage if they did not contain detectable peaks (peak area-to-noise ratio, > 5:1) for the prostatic metabolites (choline, creatine, and citrate) (Fig. 2) or if the voxels contained broad metabolite peaks (waterline width, > 20 Hz) in the regions of T1-weighted artifact. The number of voxels with degraded spectra and the total number of voxels in the peripheral zone were recorded for each patient.

Lipid contamination and motion artifact may also result in spectral degradation but are associated with distinctive features (Fig. 3). Large lipid peaks are a feature of spectral degradation due to periprostatic lipid contamination. Broad water- and metabolite-line widths throughout the 3D MR spectroscopic imaging data set are features of spectral degradation due to motion artifact.

Statistical Analysis

All statistical analysis was performed using SAS software version 8.2 (SAS Institute). A p value of less than 0.05 was considered statistically significant. We assessed interobserver agreement of reviews on the basis of sextant results. Kappa statistics were calculated using generalized estimation equations to adjust for the correlation among sextants from the same subjects. Spearman's rank correlation was used for ordinal hemorrhage scores for each sextant. The analysis of MRI results was based on a per-sextant analysis (i.e., the outcome variable of per-sextant capsular irregularity was correlated with the predictor variables of time from biopsy and degree of per-sextant postbiopsy hemorrhage using a linear regression analysis). The analysis of MR spectroscopic imaging results was based on a per-prostate analysis (i.e., the outcome variable of percentage voxels with degraded spectra in the peripheral zone was correlated with the predictor variables of time from biopsy and degree of hemorrhage [total hemorrhage in peripheral zone] using Spearman's rank correlation and Wilcoxon's rank sum tests, respectively). Per-voxel or per-sextant analysis of hemorrhage score with MR spectroscopic imaging was not performed because of the limitation of misregistration of the spectroscopic voxels with T1- and T2-weighted images. The MR spectroscopic data were not obtained from identical levels to T1- and T2-weighted images and were subject to partial volume averaging effect from adjacent tissue; therefore, we correlated total peripheral zone hemorrhage with the total percentage of degraded spectra in the entire peripheral zone.

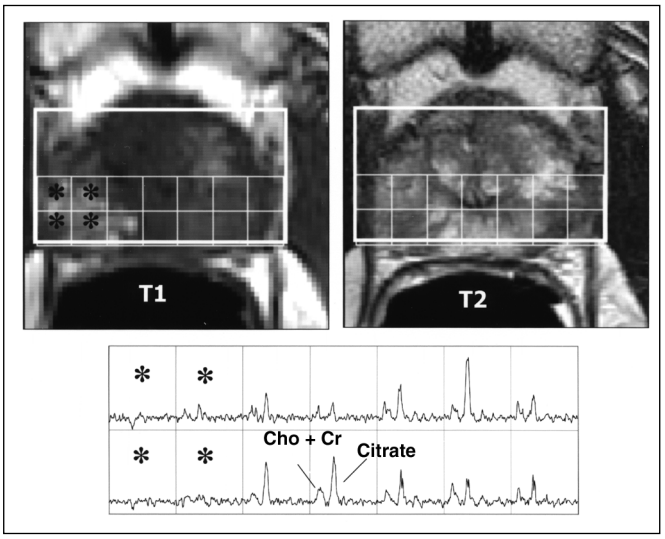

Fig. 2.—58-year-old man with mean prostate-specific antigen level of 6.3 ng/mL and positive transrectal biopsy indicating Gleason-score-6 tumor at left lateral apex. Axial T1-weighted image (TR/TE, 700/8) shows high-signal-intensity hemorrhage in right apex and spectral degradation in voxels (*asterisks*) from this region. Voxels adjacent to regions of hemorrhage show normal metabolic spectra, even though one voxel contains some high-signal-intensity change on T1-weighted image. Low-signal-intensity change is present in peripheral zone bilaterally on T2-weighted image. Cho = choline, Cr = creatine.

Results

There was good interobserver agreement for hemorrhage scores (Spearman's rank correlation coefficients for per-sextant reviewer hemorrhage scores ranged from 0.55 to 0.75). The extent of postbiopsy hemorrhage on T1-weighted images was inversely related to time from biopsy ($p < 0.01$); the mean total postbiopsy hemorrhage score per patient was 39.3 ($n = 27$) within 8 weeks of biopsy and 5.1 ($n = 16$) after 8 weeks (Fig. 4).

The two reviewers identified capsular irregularity in 36 (14%) and 30 (12%) of 258 sextants, respectively ($\kappa = 0.45$). Reviewers did not identify loss of rectoprostatic angle, neurovascular bundle enlargement, or seminal vesicle invasion in any patient. The observation of capsular irregularity was not related to the time from biopsy or

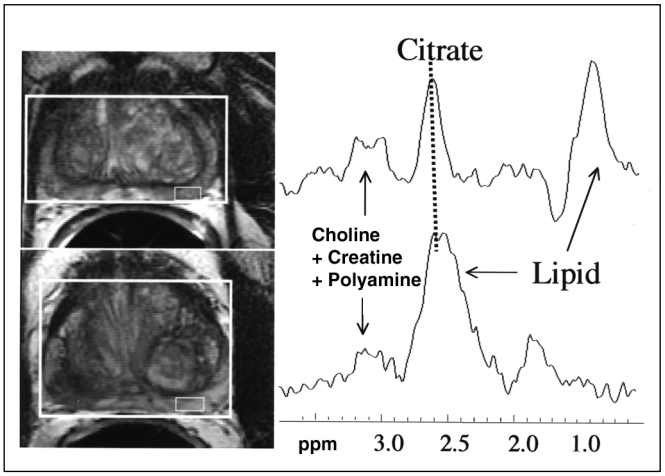

Fig. 3.—Patterns of spectral degradation from lipid contamination and motion artifact. Top image is from 65-year-old man with negative findings on prostate biopsy, and bottom image is from 68-year-old man with Gleason-score-6 tumor at right base. Spectra on top are obtained from left base location (*small rectangle*) of adjacent T2-weighted axial image (TR/TE_{eff}, 5,000/96) and are examples of spectral degradation from periprostatic lipid contamination as shown by presence of large lipid peak. Spectra on bottom are obtained from left base location (*small rectangle*) of adjacent T2-weighted axial image (5,000/96) and are examples of spectral degradation from motion artifact as shown by broad metabolite peaks and frequency shift of lipid peak that overlaps citrate peak.

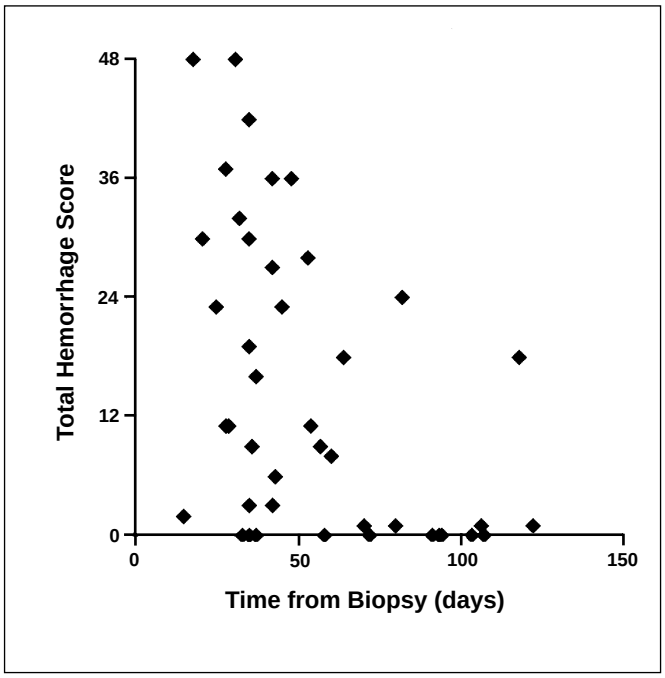

Fig. 4.—Graph shows correlation of total hemorrhage score after biopsy with time (days) from prostate biopsy.

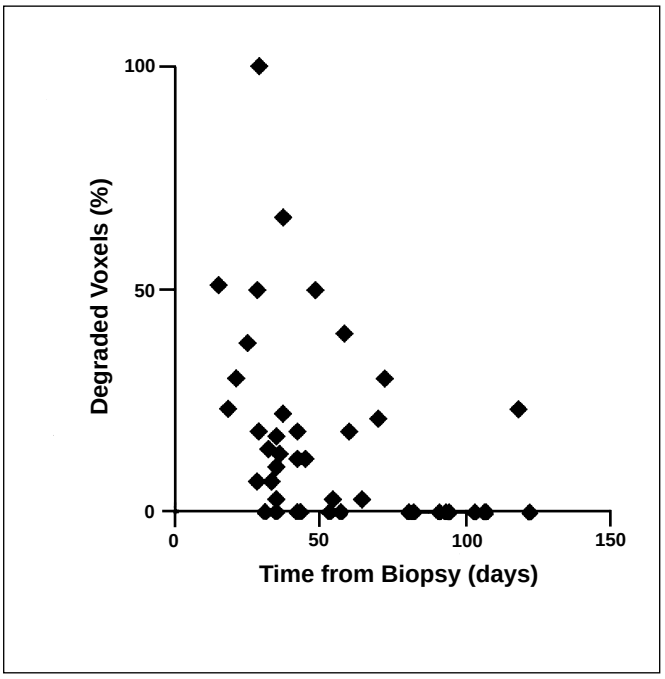

Fig. 5.—Graph shows correlation of spectrally degraded voxels with time (days) from biopsy.

degree of visible postbiopsy hemorrhage in the sextant on T1-weighted images ($p > 0.05$).

Spectral degradation was inversely related to time from biopsy ($p < 0.01$) (Fig. 5); the mean percentage of degraded voxels was 18.5% in patients imaged within 8 weeks of biopsy compared with 7% in patients imaged more than 8 weeks after biopsy. Spectral degradation was not related to total hemorrhage score ($p = 0.37$) (Fig. 6).

Discussion

Our study provides several important results related to the performance and interpretation of endorectal MRI and MR spectroscopic imaging of the prostate after biopsy. We did not observe a significant relationship between capsular irregularity and the time interval from biopsy or the degree of hemorrhage on T1-weighted images. Capsular irregularity is considered an important MRI sign of extraprostatic tumor extension [3, 10, 11, 21–28]; however, it has been suggested that capsular changes may be related to trauma, including prostatic biopsy [12]. Other features of local disease extension, such as loss of the rectoprostatic angle, neurovascular bundle enlargement, and seminal vesicle invasion [2, 5, 12, 17, 29, 30], were not observed in our patient population with organ-confined disease and may be more specific. Our study suggests that less specific capsular changes are common in organ-confined prostate cancer and are unrelated to time from biopsy and extent of postbiopsy hemorrhage; these findings suggest that these changes may represent a normal variant rather than a biopsy artifact.

Spectral degradation was found to be unrelated to the presence of visible postbiopsy hemorrhage on T1-weighted images but was significantly more frequent within the first 8 weeks after transrectal biopsy. This finding suggests that although postbiopsy hemorrhage and spectral degradation can occur together, postbiopsy change other than visible hemorrhage on T1-weighted images may be responsible for spectral degradation. The presence of postbi-

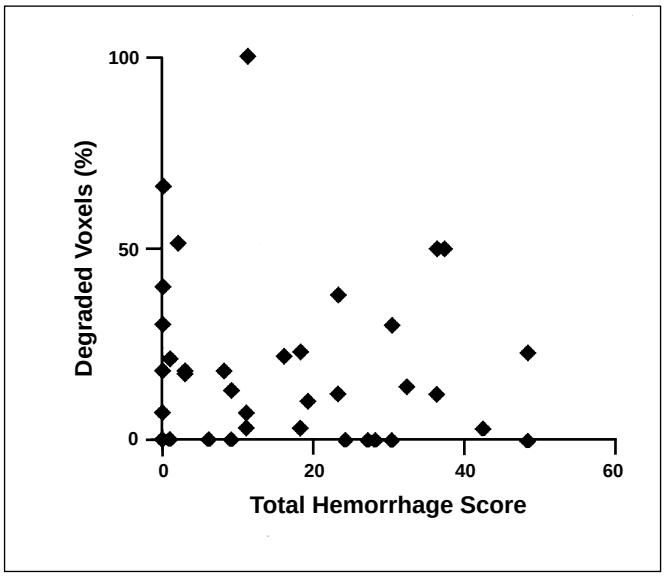

Fig. 6.—Graph shows correlation of spectrally degraded voxels with extent of visible hemorrhage.

opsy hemorrhage on T1-weighted images is considered important because of the potential to over- or underestimate tumor extent or stage on MRI and MR spectroscopic imaging [12]. The inverse correlation of time from biopsy with spectral degradation in our study suggests that an interval of 8 weeks between MRI and MR spectroscopic imaging may be beneficial, rather than the previously recommended interval of 3 weeks [2, 12–14]. Such an increase in postbiopsy interval for optimal MRI and MR spectroscopic imaging would need to be balanced against patient anxiety, although this interval is probably negligible in terms of the natural history of prostate cancer.

Limitations of our study include the use of a patient population with organ-confined disease, which prevents assessment of the capsule appearances in patients with local tumor extension. In addition, we did not localize tumor nodules in this study because our purpose was to determine whether prostate capsule irregularity occurs in patients with organ-confined prostate cancer and to determine the impact of biopsy interval rather than local tumor staging on MR spectroscopic imaging. In a study of patients imaged within and after 3 weeks of biopsy, White et al. [12] showed a reduction in reviewer accuracy in the presence of postbiopsy hemorrhage within 3 weeks of biopsy. MRI and MR spectroscopic imaging are not routinely performed before prostate biopsy in patients suspected of having prostate cancer for logistic and economic reasons, and we could not evaluate patients with MRI and MR spectroscopic imaging performed before transrectal biopsy to confirm that the capsular changes were unrelated to any biopsy trauma or to determine the number of degraded voxels occurring in patients without biopsy. However, spectral degradation was inversely related to time from biopsy suggesting a causal relationship. Prostate biopsies were performed with variable techniques at a number of institutions rather than using a single standard institutional approach; this practice reflects the usual patient-referral procedure for preoperative MRI and MR spectroscopic imaging. However, the lack of a temporal relationship between capsular findings and biopsy indicates that capsular irregularity may not be related to prostate biopsy, irrespective of the technique. Localization of exact biopsy sites on imaging was not possible because of the limitations of accurate documentation of biopsy position inherent in the transrectal sonographic technique. Correlation of capsular irregularity on imaging with biopsy location and histopathologic findings is also difficult because they are not contemporaneous. Some overlap between hemorrhage grade and sextant localization is likely to have occurred because these observations are qualitative by nature, although the total number of abnormal sextants should not be affected.

In conclusion, in patients with organ-confined prostate cancer, capsular irregularity can be seen at any time after biopsy and is independent of the degree of hemorrhage, whereas spectral degradation is seen predominantly in the first 8 weeks after biopsy. MRI staging criteria and guidelines for scheduling studies after biopsy may require appropriate modification.

References

1. American Cancer Society, Inc. Estimated new cancer cases and deaths by gender: US 2004. *Cancer Facts and Figures* 2004:4
2. Cheng D, Tempany MC. MR imaging of the prostate and bladder. *Semin Ultrasound CT MR* 1998;19:67–89
3. Kurhanewicz J, Vigneron DB, Males RG, Swanson MG, Yu KK, Hricak H. The prostate gland: a clinically relevant approach to imaging. *Radiol Clin North Am* 2000;38:116–138
4. D'Amico AV, Whittington R, Malkowicz SB, et al. A multivariate analysis of clinical and pathological factors that predict for prostate specific antigen failure after radical prostatectomy for prostate cancer. *J Urol* 1995;154:131–138
5. Yu KK, Scheidler J, Hricak H, et al. Prostate cancer: prediction of extracapsular extension with endorectal MR imaging and three-dimensional proton MR spectroscopic imaging. *Radiology* 1999;213:481–488
6. D'Amico AV, Whittington R, Malkowicz SB, et al. Combined modality staging of prostate carcinoma and its utility in predicting pathologic stage and postoperative prostate specific antigen failure. *Urology* 1997;49:23–30
7. Soulie M, Aziza R, Escourrou G, et al. Assessment of the risk of positive surgical margins with pelvic phased-array magnetic resonance imaging in patients with clinically localized prostate cancer: a prospective study. *Urology* 2001;58:228–232
8. Kurhanewicz J, Vigneron DB, Nelson SJ. Three-dimensional magnetic resonance spectroscopic imaging of brain and prostate cancer. *Neoplasia* 2000;2:166–189
9. Vigneron DB, Males R, Hricak H, et al. Prostate cancer: correlation of 3D MRSI metabolite levels with histologic grade (abstr). *Radiology* 1998;209(P):181
10. Chelsky MJ, Schnall MD, Seidmon EJ, Pollack HM. Use of endorectal surface coil magnetic resonance imaging for local staging of prostate cancer. *J Urol* 1993;150:391–395
11. Schnall MD, Imai Y, Tomaszeeoski J, Pollack HM, Lenkinski RE, Kressel HY. Prostate cancer: local staging with endorectal surface coil MR imaging. *Radiology* 1991;178:797–802
12. White S, Hricak H, Forstner R, et al. Prostate cancer: effect of post-biopsy hemorrhage on interpretation of MR images. *Radiology* 1995;195:385–390
13. Ramchandani P, Schnall MD. Magnetic resonance imaging of the prostate. *Semin Roentgenol* 1993;28:74–82
14. Ikonen S, Kivisaari L, Vehmas T, et al. Optimal timing of post-biopsy MR imaging of the prostate. *Acta Radiol* 2001;42:70–73
15. Bauer JJ, Zeng J, Zhang W, et al. Lateral biopsies added to the traditional sextant prostate biopsy pattern increases the detection rate of prostate cancer. *Prostate Cancer Prostatic Dis* 2000;3:43–46
16. Kurhanewicz J, Vigneron DB, Hricak H, Narayan P, Carroll P, Nelson SJ. Three-dimensional H-1 MR spectroscopic imaging of the in situ human prostate with high (0.24-0.7cm^3) spatial resolution. *Radiology* 1996;198:795–805
17. Yu KK, Hricak H, Alagappan R, Chernoff DM, Bacchetti P, Zaloudek CJ. Detection of extracapsular extension of prostate carcinoma with endorectal and phased-array coil MR imaging: multivariate feature analysis. *Radiology* 1997;202:697–702
18. Kurhanewicz J, Vigneron DB, Males RG, Swanson MG, Yu KK, Hricak H. The prostate: MR imaging and spectroscopic imaging—present and future. *Radiol Clin North Am* 2000;38:115–138
19. Star-Lack J, Nelson SJ, Kurhanewicz J, Huang LR, Vigneron DB. Improved water and lipid suppression for 3D PRESS CSI using RF band selective inversion with gradient dephasing (BASING). *Magn Reson Med* 1997;38:311–321
20. Tran TK, Vigneron DB, Sailasuta N, et al. Very selective suppression pulses for clinical MRSI studies of brain and prostate cancer. *Magn Reson Med* 2000;43:23–33
21. Hricak H, White S, Vigneron D, et al. Carcinoma of the prostate gland: MR imaging with pelvic phased-array coils versus integrated endorectal-pelvic phased-array coils. *Radiology* 1994;193:703–709
22. Quinn SF, Franzini DA, Demlow TA, et al. MR imaging of prostate cancer with an endorectal surface coil technique: correlation with whole-mount specimens. *Radiology* 1994;190:323–327
23. Tempany CM, Zhou X, Zerhouni EA, et al. Staging of prostate cancer: results of Radiology Diagnostic Oncology Group project comparison of three MR imaging techniques. *Radiology* 1994;192:47–54
24. Gibbons RP, Correa RJ Jr, Brannan GE, Weissman RM. Total prostatectomy for clinically localized prostate cancer: long-term results. *J Urol* 1989;141:564–566
25. Chodak GW, Thisted RA, Gerber GS, et al. Results of conservative management of clinically localized prostate cancer. *N Engl J Med* 1994;330:242–248
26. Fair WR, Aprikian A, Sogani P, Reuter V, Whitmore WF Jr. The role of neoadjuvant hormonal manipulation in localized prostatic cancer. *Cancer* 1993;71:1031–1038
27. Gibbons RP, Cole BS, Richardson RG, et al. Adjuvant radiotherapy following radical prostatectomy: results and complications. *J Urol* 1986;135:65–68
28. Hricak H, Dooms GC, Jeffrey RB, et al. Prostate carcinoma: staging by clinical assessment, CT, and MR imaging. *Radiology* 1987;162:331–336
29. Outwater EK, Peterson RO, Siegelman ES, Gomella LG, Chernesky CE, Mitchell DG. Prostate carcinoma: assessment of diagnostic criteria for capsular penetration on endorectal coil MR images. *Radiology* 1994;193:333–339
30. Coakley FV, Kurhanewicz J, Lu Y, et al. Prostate cancer tumor volume: measurement with endorectal MR and MR spectroscopic imaging. *Radiology* 2002;223:91–97